JOURNAL OF GEOPHYSICAL RESEARCH: ATMOSPHERES, VOL. 118, 1123–1138, doi:10.1002/jgrd.50137, 2013

Deuterium excess variations of rainfall events in a coastal area of South Australia and its relationship with synoptic weather systems and atmospheric moisture sources

Huade Guan,[1,2,3] Xinping Zhang,[3] Grzegorz Skrzypek,[4] Zhian Sun,[5] and Xiang Xu[1,2]

Received 24 April 2012; revised 21 December 2012; accepted 26 December 2012; published 31 January 2013.

[1] In this study, isotopic compositions of monthly (Global Network of Isotopes in Precipitation), event, and intraevent rain samples are used to examine the relationship between precipitation deuterium excess, the type of synoptic weather systems, and associated moisture directions in a coastal area of South Australia. The results indicate that both synoptic weather systems and associated atmospheric moisture sources influence deuterium excess values in precipitation. Rain events caused by frontal systems tend to have moisture sources from the Indian Ocean to the south of Australia. They usually have deuterium excess values of 15‰ to 25‰, depending on the moisture source direction. Rain events caused by synoptic low-pressure and trough systems tend to have inland moisture sources, and have a deuterium excess of 10‰ to 15‰. In addition to weather systems and associated moisture sources, subcloud processes alter the deuterium excess in the resulting precipitation, which is an effect that is more significant during summer when it is warm and dry. Together, these factors contribute to the seasonal variability of deuterium excess in the study area. Deuterium excess of winter frontal precipitation, resulting from minimal subcloud evaporation, is useful to infer the moisture source direction. In other seasons, deuterium excess in precipitation is more likely altered by subcloud evaporation. Nevertheless, intraevent samples in the middle of a frontal event that has experienced minimal subcloud evaporation are useful to estimate cloud deuterium excess. The results also suggest that an abrupt change in dominant precipitation weather patterns occurs between January and February, characterized by a sudden decrease in $\delta^{18}O$ and deuterium excess.

Citation: Guan, H., X. Zhang, G. Skrzypek, Z. Sun, and X. Xu (2013), Deuterium excess variations of rainfall events in a coastal area of South Australia and its relationship with synoptic weather systems and atmospheric moisture sources, *J. Geophys. Res. Atmos.*, *118*, 1123–1138, doi:10.1002/jgrd.50137.

1. Introduction

[2] The stable hydrogen and oxygen isotopic composition (δ^2H and $\delta^{18}O$) of water provides valuable information to trace hydrological processes on land [*Allison and Barnes*, 1983; *Gat and Alrey*, 2006; *Blasch and Bryson*, 2007; *Frot et al*., 2007], in the atmosphere [*Worden et al*., 2007; *Bony et al*., 2008; *Risi et al*., 2008a; *Barras and Simmonds*, 2009; *Frankenberg et al*., 2009; *Yoshimura et al*., 2010], and between land and the atmosphere [*Gat*, 1996; *Yakir and Sternberg*, 2000] at regional and global scales [*Salati et al*., 1979; *Gat and Matsui*, 1991; *Yoshimura et al*., 2004; *Risi et al*., 2010c] and at a local scale [*Moreira et al*., 1997; *Yepez et al*., 2003; *Williams et al*., 2004; *Wang et al*., 2010]. The isotopic composition of the paleoprecipitation stored in authigenic materials is useful to infer paleoclimate and other past environmental conditions [*Dangela and Longinelli*, 1990; *Rozanski et al*., 1997; *Thompson et al*., 2000; *Jouzel*, 2003; *McCarroll and Loader*, 2004; *McDermott*, 2004; *Blisniuk and Stern*, 2005; *Wang et al*., 2006]. A quantitative understanding of the controls on precipitation isotope composition and its variations is required for isotopic applications in these areas.

[3] Variations in δ^2H and $\delta^{18}O$ values of precipitation water result from both equilibrium and kinetic fractionations depending on many factors and processes. These processes include conditions of moisture source areas, moisture transport trajectories, precipitation histories, weather systems leading to precipitation, and subcloud processes. Thus, the isotopic composition is highly variable when it is measured in precipitation over a short term (e.g., monthly, or even daily and event-based) [*Yoshimura et al*., 2010; *Vodila et al*., 2011]. When

[1]School of the Environment, Flinders University of South Australia, Australia.
[2]National Centre for Groundwater Research and Training, Adelaide, Australia.
[3]College of Resource and Environmental Science, Hunan Normal University, Changsha, Hunan, China.
[4]West Australian Biogeochemistry Centre, School of Plant Biology, The University of Western Australia, Perth, Western Australia, Australia.
[5]Centre for Australian Weather and Climate Research, Melbourne, Victoria, Australia.

Corresponding author: Dr. H. Guan, School of the Environment, Flinders University, Adelaide, South Australia, Australia. (huade.guan@flinders.edu.au)

2169-897X/13/10.1002/jgrd.50137

these temporal variations are resolved, they will become useful to better understand the atmospheric processes during precipitation events that may otherwise be unobservable [*Yoshimura et al*., 2010]. Thus, isotope-incorporated atmospheric general circulation models and regional climate models have been developed to include isotope information in the system [*Joussaume et al*., 1984; *Jouzel et al*., 1997; *Hoffmann et al*., 1998; *Noone and Simmonds*, 2002]. The second-order isotopic variable, deuterium excess (details to be given later), is thought to be highly sensitive to the physical processes that generate strong kinetic effects, such as condensation at supersaturation and evaporation, providing an additional constraint to examine the capacity of model representation of these processes. However, some isotope-incorporated atmospheric models are reported to have difficulties in capturing observed deuterium excess [*Werner et al*., 2001; *Mathieu et al*., 2002; *Lee et al*., 2007; *Risi et al*., 2010a], which suggests that our understanding of the processes controlling deuterium excess and their representation in general circulation models needs to be improved.

[4] The Global Network of Isotopes in Precipitation (GNIP) joint program between the International Atomic Energy Agency and the World Meteorological Organisation, and other regional monitoring networks, have greatly improved our knowledge of the precipitation isotopic composition and its relationship with environmental variables (or isotope transfer functions, ITFs) [*Dansgaard*, 1964]. The ITFs derived from measurements, primarily relating isotopic compositions of precipitation to air temperature and precipitation amounts [*Dansgaard*, 1964; *Rozanski et al*., 1992], have been used to study paleoclimate and climate (in particular, air temperature) changes from precipitation and other terrestrial isotope archives (ice cores, speleothems, groundwater, tree rings, bone, and tooth, etc.) [*Rozanski et al*., 1997; *Jouzel*, 2003; *McCarroll and Loader*, 2004; *McDermott*, 2004; *Skrzypek et al*., 2011]. These ITFs are generally based on relatively long temporal records or spatially distributed observations [*Kohn and Welker*, 2005], and have been used to examine a possible change of mean conditions. However, these ITFs tend to be site-specific [*Jones et al*., 2009], and may vary with a temporal change of the climate system [*Krinner et al*., 1997; *Sime et al*., 2009; *Field*, 2010; *Masson-Delmotte et al*., 2011]. The precipitation ITFs, such as the temperature effect, may vary if the moisture sources for precipitation are different [*Masson-Delmotte et al*., 2008; *Ersek et al*., 2010; *Vachon et al*., 2010]. Meanwhile, changes in the occurrence of large-scale weather patterns in the past can be revealed from precipitation isotopic composition if it is distinctive between precipitation events resulting from different circulation patterns that often involve different moisture sources. Thus, it is necessary to separate the effects of moisture sources from other environmental variables on precipitation isotopic compositions. Deuterium excess has been shown to be useful for such analyses [*Masson-Delmotte et al*., 2008].

[5] Precipitation isotopic composition, resulting from complex atmospheric processes, provides the necessary inputs to trace subsequent terrestrial hydrological processes. However, long-term records of precipitation isotopic composition are only available from the sparse GNIP network in most areas. This network is insufficient to resolve the spatial variability of precipitation isotopic composition at the catchment scale [*Guan et al*., 2009], which is needed to investigate hydrological processes at this small spatial scale. Some efforts have been made to geostatistically interpolate the GNIP observations to spatially continuous precipitation isotopic composition maps [*Bowen and Wilkinson*, 2002; *Bowen and Revenaugh*, 2003], in which some geographic patterns of precipitation isotopic composition are incorporated. These geographic patterns lump the isotopic effects of various processes. They often only apply when the precipitation isotopic composition is averaged over a long period and for a relatively coarse spatial resolution. Such statistical methods have difficulty in representing dynamic and fine-resolution variabilities. A large portion of this small-scale spatial variability in precipitation isotopes is associated with the subcloud processes (moisture exchange and raindrop re-evaporation) [*Liotta et al*., 2006; *Guan et al*., 2009]. If the effects of these subcloud processes on precipitation isotopic composition can be quantified, it is possible to spatially extrapolate the precipitation isotope composition at one GNIP site to the surrounding area. Thus, from the aspect of using water isotopes in investigating terrestrial hydrological processes, there is also a need to separate the effects of various processes that influence precipitation isotopic composition.

[6] The secondary isotopic variable, deuterium excess, has been demonstrated to be useful in inferring moisture sources and subcloud processes [*Masson-Delmotte et al*., 2005; *Liotta et al*., 2006; *Zhang et al*., 2010; *Lai and Ehleringer*, 2011]. In comparison to individual isotopic composition, deuterium excess (d), defined in equation (1) [*Dansgaard*, 1964], is less variable, by cancelling out the covariation of oxygen and hydrogen isotopic compositions during the equilibrium fractionation.

$$d = \delta^2 H - 8 \cdot \delta^{18} O \tag{1}$$

[7] The in-cloud Rayleigh process tends to slightly increase deuterium excess of the condensate from that of the cloud vapor, and the difference gradually decreases with an increase of rainout fraction (Figures 1a and 1b). The rainout process does not result in a large variation of precipitation deuterium excess if the equilibrium temperature is constant (Figure 1a), but temperature variation during the equilibrium fractionation can lead to some change in d-excess of the resultant precipitation [*Pfahl and Wernli*, 2008]. For example, a variation of 5°C in equilibrium condensation temperature can lead to a change of deuterium excess of 2‰ (Figure 1b). This situation more likely happens in a convective event in which condensation may occur over a large vertical distance. Deuterium excess is more sensitive to kinetic fractionation processes [*Masson-Delmotte et al*., 2008]. These processes occur at the moisture source areas (e.g., ocean evaporation), in the cloud (e.g., condensation in supersaturation conditions), and in the subcloud layer (e.g., re-evaporation, moisture exchange with ambient air). Examination of deuterium excess in precipitation will help in understanding these processes. However, in comparison to δ^2H and δ^{18}O, deuterium excess is much more rarely studied.

[8] The global average d-excess in precipitation is 10‰ [*Craig*, 1961], which is attributed to evaporation from an average ocean surface with a sea surface temperature (SST) of 25°C, and a relative humidity (RH) of 80% [*Merlivat and Jouzel*, 1979]. The vapor d-excess at the ocean surface is negatively correlated with RH and slightly

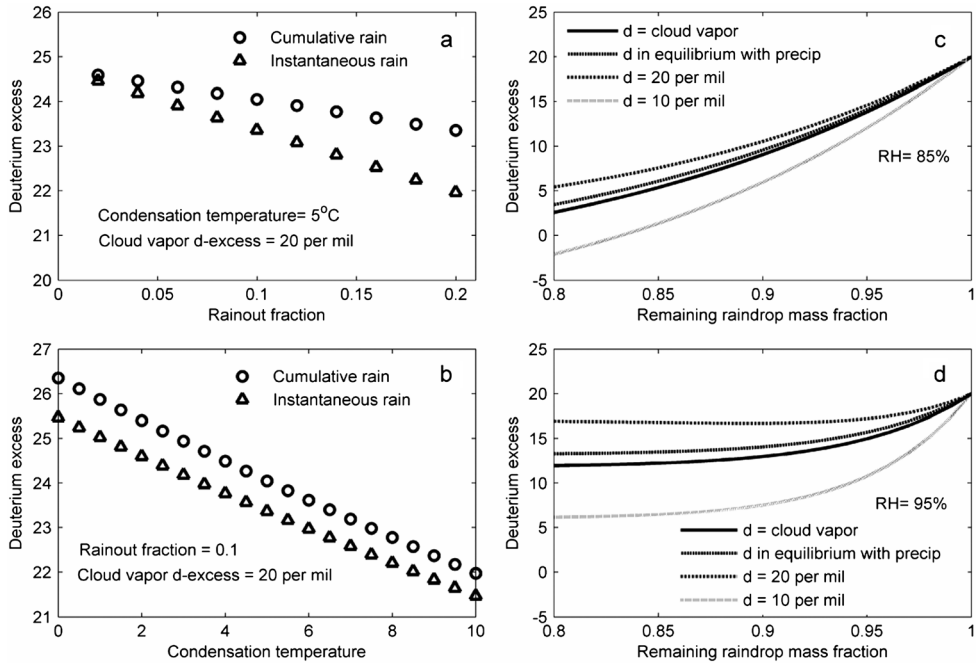

Figure 1. Precipitation deuterium excess resulting from in-cloud Rayleigh process as a function of rainout fraction (a) and cloud-base temperature (b), and from subcloud evaporation and moisture exchange as a function of raindrop evaporation fraction for an ambient subcloud air with an average RH of 85% (c) and 95% (d), for four selected *d*-excess values for subcloud vapor. For Figures 1a and 1b, it is assumed that the cloud vapor has a deuterium excess of 20‰, and a $\delta^{18}O$ of −15‰. For Figures 1c and 1d, it is assumed that precipitation at the cloud base (1000 m above ground) has a deuterium excess of 20‰ (the equilibrium cloud vapor deuterium excess is calculated as 17.6 ‰), and a $\delta^{18}O$ of −5‰. The effective RH and temperature are assumed to be an average temperature and RH between ground surface (T = 15°C, RH = 70% or 90%) and cloud base (RH = 100%, temperature calculated from a lapse rate of −6.5°C/km). The results are calculated by the authors from the Stewart model [*Stewart*, 1975], with diffusion parameter values adopted from [*Cappa et al*., 2003].

positively correlated with SST [*Pfahl and Wernli*, 2008; *Uemura et al*., 2008]. Thus, the spatial variability of sea surface condition–dependent *d*-excess provides a signature map, potentially useful to match the moisture sources for precipitation [*Yamanaka et al*., 2002; *Pang et al*., 2005].

[9] The precipitation *d*-excess is also dependent on other processes, in particular, the subcloud evaporation and moisture diffusive exchange. Subcloud evaporation (i.e., re-evaporation of the falling raindrops) and moisture exchange with the ambient air in the subcloud layer are common processes altering rain isotopic composition [*Liebminger et al*., 2006; *Peng et al*., 2007; *Guan et al*., 2009; *Yoshimura et al*., 2010]. The isotope composition of residual raindrops resulting from subcloud processes can be estimated by Stewart's equation [*Stewart*, 1975], which was used for describing the relationship between *d*-excess and loss of mass from raindrops falling through the subcloud layer of different properties (Figures 1c and 1d). Subcloud evaporation and moisture exchange tends to decrease *d*-excess in the residual rainwater. In situations in which deuterium excess in the subcloud layer is larger than that of raindrops, moisture exchange may lead to an increase of deuterium excess in the resultant precipitation. The subcloud evaporation effect increases with the evaporation fraction. Evaporation of 5% at a RH of 85% in the subcloud layer (or 70% at the ground level in Figure 1c, in which an effective RH is assumed to be an average of those at the ground level and at the cloud base) may decrease deuterium excess from an initial 20‰ to approximately 15‰ in precipitation water. A larger evaporation fraction further decreases *d*-excess of the resultant rainfall. Moisture exchange with the ambient vapor tends to reduce evaporation effects on the *d*-excess of the residual raindrops, with the magnitude depending on the ambient vapor isotope composition and RH in the subcloud layer (Figures 1c and 1d). For a subcloud layer with a larger RH (e.g., 95%), isotope exchange becomes more important. The deuterium excess of the resultant precipitation is dependent on the isotopic composition of the ambient vapor in the subcloud layer. As a result from the subcloud processes, *d*-excess of the raindrops may be altered during precipitation. In addition, moisture recycling and mixing during precipitation alter the isotopic signatures of vapor in both the cloud and subcloud layers, in particular during a convective event [*Bony et al*., 2008], complicating the pattern of isotope composition and deuterium excess in the resultant precipitation.

[10] In Australia, data from six GNIP sites show that deuterium excess is greater than the global average value (10‰) [*Liu et al*., 2010]. The *d*-excess is larger in austral winter (June–August) than in summer (December–February). The seasonal variation of precipitation *d*-excess at the Adelaide GNIP site is shown in Figure 2b. This seasonal variation

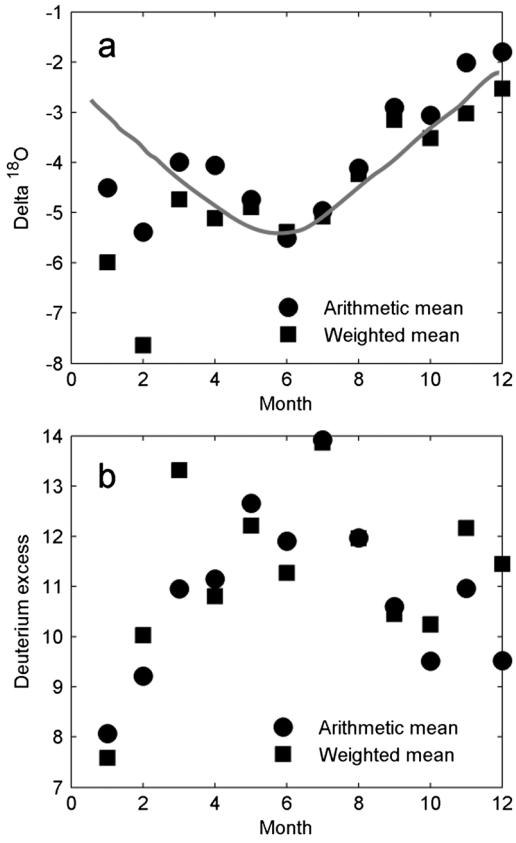

Figure 2. Arithmetic mean and weighted mean monthly $\delta^{18}O$ (a) and deuterium excess (b) at the Adelaide GNIP site (#9467500, 34.97°S, 138.58°E), with data duration of about 10 years, collected between 1962 and 1984. The gray curve in Figure 2a is hand-drawn to approximately represent a hypothetical gradual change of monthly precipitation isotopic composition.

has been attributed to a high RH in the moisture source ocean surface for summer precipitation [*Liu et al.*, 2010]. However, other factors, as discussed previously, may contribute to this seasonal pattern. For example, it is likely that the low *d*-excess in summer rain is a result of subcloud processes due to a warm and dry climate, or because the moisture source area is different from the winter precipitation and has a low *d*-excess. Thus, a gradual change in climatic average of monthly moisture sources, source area conditions, or subcloud processes, can all potentially result in a gradual change of seasonal precipitation isotopic composition (e.g., the gray curve in Figure 2a). However, an abrupt change in precipitation isotopic composition for January and February at the Adelaide GNIP site (Figure 2a) suggests that there are some factors other than a gradual seasonal change controlling precipitation isotopic composition. A recent study on the spatial patterns of long-term average monthly precipitation in Adelaide and the surrounding area shows that February rainfall is much less dependent on orographic variables than other months [*Guan et al.*, 2009]. This may be related to the different dominant synoptic weather systems in this month compared with the rest of the year. This difference in synoptic weather systems may abruptly change the moisture source and/or in-cloud and subcloud processes, leading to both low *d*-excess and $\delta^{18}O$ values, such as those in January and February at the Adelaide GNIP site (Figure 2). Examination of event isotope data is helpful to understand the isotopic effects of these processes [*Celle-Jeanton et al.*, 2004; *Barras and Simmonds*, 2009; *Yoshimura et al.*, 2010].

[11] The objectives of this study are to examine (1) event precipitation deuterium excess in a coastal area of South Australia, (2) whether precipitation deuterium excess varies systematically and predictably with synoptic weather systems and associated moisture source directions, (3) the primary factors influencing seasonal variability of precipitation deuterium excess, and (4) potential mechanisms leading to both low *d*-excess and $\delta^{18}O$ in summer precipitation in the study area. The results of this work will provide valuable information to understanding the processes controlling precipitation deuterium excess in the study area, which will also be useful for similar coastal areas that are influenced by both oceanic and continental air masses.

2. Methodology

2.1. Study Area

[12] The study is based on Adelaide and the Mount Lofty Ranges (Figure 3). Adelaide (34.93°S, 138.58°E) is the capital city of South Australia. It is bounded on the west by St Vincent Gulf, and on the east by the Mount Lofty Ranges. St Vincent Gulf is about 150 km long and 70 km

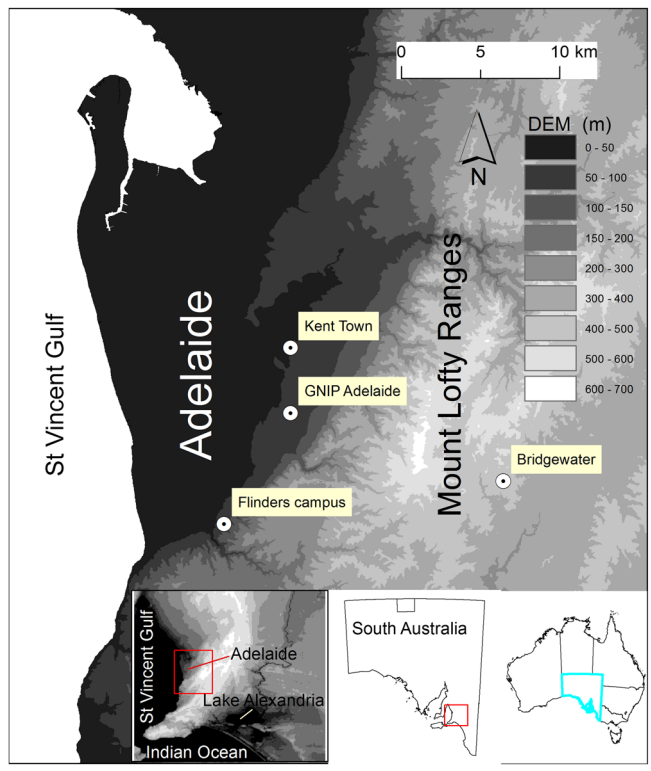

Figure 3. The study area showing the location of two sites of event rainwater collection (the Flinders University campus 160 m a.s.l. and Bridgewater 435 m a.s.l.), one GNIP site, and one reference BOM weather station (Kent Town). The nearby water bodies are marked in one inset map.

wide, and is connected to the Great Australian Bight, an open bay to the south of Australia in the Indian Ocean. The Mount Lofty Ranges are a series of small mountain ranges with moderate topographic relief of less than 700 m a.s.l. To the south of the study area is the Indian Ocean, with Lake Alexandria located 80 km to the southwest. The lake has an area of 650 km^2, and an average water depth of 2.8 m. Within 80 km distance from the study site, the ocean surface has an area of approximately 7000 km^2. The prevailing wind direction at the study site is southwesterly (in summer) to northwesterly (in winter) during the daytime, and easterly (in summer) to northerly (in winter) during the nighttime [*Guan et al.*, 2012], indicating that the lake evaporation vapor is not transported to the study site during most times of the year. Thus, the effect of local lake evaporation on the isotopic composition of precipitation is considered not important. The study area is connected inland to the north. The climate is of a Mediterranean type, with a wet winter and a dry summer. Long-term (1977–2011) average annual precipitation measured at Kent Town (elevation, 48 m a.s.l.) by the Bureau of Meteorology, near the study area, is approximately 550 mm (Figure 4). Mean monthly maximum temperature occurs in February (29.4°C), and mean monthly minimum temperature (7.5°C) happens in July (http://www.bom.gov.au/climate/data/, accessed on January 2012).

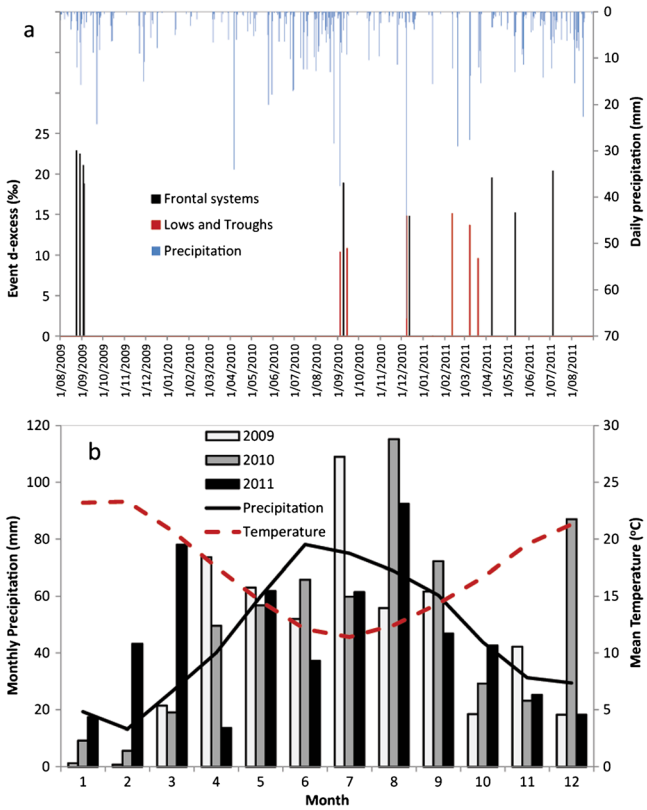

Figure 4. (a) Precipitation *d*-excess for rainfall events collected for isotopic analyses, in comparison to daily precipitation measured at BOM station 23090 (Kent Town). (b) Monthly precipitation of 2009, 2010, and 2011, in comparison to long-term (1977–2011) mean precipitation at Kent Town. Mean monthly temperature is also shown.

2.2. Rainwater Collection and Isotopic Analysis

[13] Event rainwater samples were collected at two sites: the Flinders University campus (elevation, 160 m a.s.l.) in Adelaide, and Bridgewater (elevation, 435 m) in the Mount Lofty Ranges (Figure 3). The sampling was not designed to represent the isotopic composition of mean rainfall, but that of different synoptic weather systems. Two sampling techniques were applied. The first one follows the design by [*Friedman et al.*, 1992]. One sample of total rainwater was collected for each event. Each collector, hereafter referred to as the event sampler, was made of 15 cm diameter funnel connected to a 1.5 L bottle. A 1 cm thick liquid paraffin (Ajax Finechem Pty. Ltd., Sydney, Australia) was applied in bottles to avoid evaporation. The funnel neck was equipped with a stainless steel mesh filter, and placed about 50 cm above the ground. The rain samples were collected as soon as the event was estimated to have finished. After the field sampling bottle was returned to the laboratory, water in the bottle was withdrawn, using a syringe to avoid oil contamination, to a clean sealed sampling bottle for storage after determining the sample volume. The second method was to use a sequential collector, in which vials were placed in a circle and rotated to collect rainwater from a tipping bucket rain gauge. The collector, hereafter referred to as the intraevent sampler, was controlled by a preprogrammed controller to collect intraevent rain samples. The timing and amount of water being collected into each vial was automatically logged. The water samples were transferred into sealed bottles within 24 h from the start of the event. No paraffin oil was used in the vials. At the early stage of the sampling period, no intraevent samplers were available. Thus, the data reported in this paper includes samples from both sampling methods at the two sites. The event isotope composition was calculated from the vial sample data. Intraevent variability of precipitation isotopic composition is shown for some selected events.

[14] Clean rainwater samples were immediately stored in a cold room at 4°C. They were filtered with 0.45 μm syringe filters before being sent to an external laboratory for stable water isotope analysis within 2 to 6 months from collection. Isotopic analysis of all samples was performed at the University of California Davis Stable Isotope Facility. This facility provided simultaneous analysis of oxygen and hydrogen isotope ratios in liquid water samples using an LGR DLT-100, Laser Absorption Spectroscopy (Los Gatos Research, Inc., Mountain View, CA, USA). Precision was reported to be 1.0‰ for δ^2H and 0.1‰ for $\delta^{18}O$.

[15] In addition to the event rain isotope data, monthly rain isotope data collected at GNIP Adelaide site (#9467500: 34.97°S, 138.58°E, 45 m a.s.l.) was also used for this study (http://isohis.iaea.org, accessed in 2008). The GNIP monthly data spans a period from 1962 to 1984, with an average of 10 years of data for each of the 12 months.

2.3. Mapping Water Vapor Deuterium Excess Over the Ocean

[16] According to *Uemura et al.* [2008], the variation of deuterium excess near the ocean surface can be largely related to SST and RH according to the following equation:

$$d = 0.45\mathrm{SST} - 0.42\mathrm{RH}* + 37.9 \quad (2)$$

where RH* is relative humidity at 15 m above sea surface

rescaled to the value at SST. NOAA Optimum Interpolation SST V2 was used in this study [*Reynolds et al*., 2002]. One degree resolution monthly SST data was acquired from NOAA/OAR/ESRL PSD, Boulder, Colorado, USA (http://www.esrl.noaa.gov/psd/). NCEP/NCAR near-surface layer monthly air temperature and relative humidity data at 2.5 degree resolution was acquired from NOAA/OAR/ESRL PSD (http://www.esrl.noaa.gov/psd/reanalysis) [*Kalnay et al*., 1996]. RH data in the surface layer was converted to that at SST for mapping.

2.4. Backward Trajectory Analysis for Moisture Sources

[17] The HYSPLIT_4 (Hybrid Single-Particle Lagrangian Integrated Trajectory) was used in this study to retrieve the backward track of the air parcel during the precipitation event [*Draxler et al*., 2009]. The origin of air masses as diagnosed from the back-trajectory analysis is assumed to approximate the moisture source direction for the water vapor and for the precipitation at the study site. The Windows-based HYSPLIT program was acquired from the Air Resource Laboratory of NOAA, USA, (http://ready.arl.noaa.gov/HYSPLIT.php). NCEP/NCAR reanalysis data were used as the meteorological data to run the HYSPLIT model, which was downloaded through the data portal provided in the HYSPLIT interface. The 4-DVAR assimilation data from the Australian Bureau of Meteorology, which included all possible meteorological observational data and operational satellite data, were also used for intercomparison. The initial fields at 12 km horizontal resolution, which were used for weather prediction in South Australia, were adopted in this study. A 48 h backward trajectory analysis was performed for each precipitation event at the study site (35°S, 138.5°E) at six levels above ground (100, 500, 1000, 2000, 3000, and 5000 m). Simultaneously, a backward trajectory analysis at the 1000 m level was performed at multiple time points in and prior to the precipitation event in order to cross-verify that the backward trajectory analysis captured the representative moisture source for the event.

2.5. Calculation of Mean Isotopic Composition

[18] Two types of mean isotopic composition calculation were used in this study. One is the amount-weighted mean, as shown in equation (3).

$$\overline{\delta_w} = \frac{\sum_{i=1}^{n} \delta_i P_i}{\sum_{i=1}^{n} P_i} \tag{3}$$

where δ_i is the isotopic composition of an individual sample with rain amount of P_i, n is the total number of these individual samples for calculating the mean isotope composition. This equation is used to calculate event isotopic compositions from intraevent samples, average event isotopic composition from the two sample sites, and multiyear mean monthly isotopic compositions from GNIP monthly data.

[19] The other is the arithmetic mean, as shown in equation (4).

$$\bar{\delta} = \frac{\sum_{i=1}^{n} \delta_i}{n} \tag{4}$$

[20] This equation is used to calculate arithmetic mean monthly isotopic compositions from GNIP data, to be compared with the weighted mean. This comparison is useful for revealing the isotopic effects of the processes playing a role during a month in which a smaller amount of precipitation has fallen.

[21] The idea is that the arithmetic mean treats the data points equally regardless of the rainfall volume, whereas the weighted mean emphasizes the data points of large rainfall amount. If the subcloud evaporation is important in a climatic month (e.g., a long-term average January), it should more likely influence the smaller events in the month, and a month (e.g., January in a specific year) with a smaller precipitation, either because the month has more small-sized events or because it is drier compared with a normal year. Thus, the subcloud evaporation should enrich $\delta^{18}O$, and decrease *d*-excess, to a larger degree for a month of smaller precipitation than the climatic average of the month. The arithmetic mean for the climatic month should then have a larger $\delta^{18}O$, and a smaller *d*-excess than the weighted mean. Thus, the comparison of both $\delta^{18}O$ and *d*-excess is helpful to examine whether the subcloud evaporation is important for a climatic month. If the means for the two quantities are the same, it suggests that the subcloud evaporation is not significant, such as those for July and August in Adelaide (Figure 2). If the subcloud evaporation is important, with an assumption that the moisture sources leading to different events in the month are the same, the two means will show systematic differences for both $\delta^{18}O$ and *d*-excess, such as those for December in Adelaide (Figure 2). For a climatic month, if the difference in $\delta^{18}O$ between the two means suggests a significant subcloud evaporation effect, whereas the arithmetic mean of *d*-excess is not smaller than the expected weighted mean (e.g., the situation for January in Figure 2b), or the difference in *d*-excess is not large enough (e.g., the situation for February in Figure 2b, in comparison to those for March and December), it indicates that the *d*-excess of a large-rainfall month is smaller than the climatic average. This can be because the weather systems, which lead to an above-average monthly precipitation, produce precipitation with a smaller *d*-excess than the climatic average of the month. One likely situation is that these weather systems have a low *d*-excess moisture source.

3. Results

[22] Altogether, 17 rainfall events were collected at the Flinders University campus (site A) and 8 rainfall events at Bridgewater (site B; Figure 3). Among them, five events were collected at both locations (Table 1). In total, 209 individual rainwater samples were analyzed during this study. All these samples were collected in August and September of 2009, and from September 2010 through July 2011 (Figure 4a), covering all four seasons. Monthly precipitation at a nearby weather station (Kent Town) in the three sampling years was compared with long-term average monthly precipitation (Figure 4b). It was significantly wetter in December 2010 and March 2011 than the long-term average.

[23] For each event, stable isotopic composition and deuterium excess are reported in Table 1, with the intraevent standard deviation of *d*-excess being included when applicable. An earlier study on the spatial distribution of deuterium excess in the study area [*Guan et al*., 2009] indicates that a systematic difference in precipitation *d*-excess exists

Table 1. Information and Isotopic Composition of 20 Event Samples Collected at the Flinders University Campus (A) and/or Bridgewater (B)

Event ID[a]	Vials[b]	Amount (mm)	T, RH (°C, %)[c]	Synoptic weather	Source Air Parcel[d]	δ^2H (‰)	$\delta^{18}O$ (‰)	d (‰)	σ (‰)[e]
A2009Aug_24	—	9.2	11, 75	Cold front	W	−22.6	−5.43	20.8	—
B2009Aug_24	—	38.4	11, 75	Cold front	W	−19.4	−5.53	24.9	—
A2009Aug_29	—	6.4	12, 73	Cold front	W	−1.4	−2.98	22.5	—
B2009Aug_29	—	6.6	12, 73	Cold front	W	−16.6	−4.90	22.6	—
A2009Sep_03	—	3.4	13, 72	Cold front	W	−13.7	−4.34	21.0	—
B2009Sep_03	—	1.8	13, 72	Cold front	W	−16.9	−4.74	21.0	—
A2009Sep_04	4	8	14, 57	Cold front	WSW	−15.9	−4.33	18.8	3.9
A2009Sep_07	—	1.8	13, 68	Cold front	WSW	−9.3	−3.22	16.4	—
B2009Sep_07	—	6	13, 68	Cold front	WSW	−14.0	−3.78	16.3	—
A2009Sep_16-17	7	14	16, 83	Low	Inland	31.3	2.55	10.9	13.4
A2009Sep_21	17	34	14, 81	Low	Inland + W	13.0	−1.46	24.7	7.7
A2009Sep_25	7	14	11, 74	Cold front	WSW	−29.5	−6.34	22	3.7
A2010Sep_03-04	18	36	11, 87	Low	Inland	−27.2	−4.70	10.4	4.7
A2010Sep_09-10	4	5.6	12, 79	Cold front	WSW	−4.0	−2.86	18.9	2.4
A2010Sep_13-14	8	14.6	13, 88	Low	Inland	−20.0	−3.85	10.8	2.5
A2010Dec_07-08	27	26.6	21, 91	Trough	Inland	−17.7	−4.05	14.8	5.6
B2010Dec_10-12	13	11.6	16, 73	Cold front	WSW	−1.3	−2.00	14.8	2.7
B2011Jan_13-14	9	14.8	21, 88	Low	Inland + S	−98.4	−12.3	0.0	8.7
A2011Feb_11	5	8.6	23, 85	Trough	Multiple directions	−26.9	−5.25	15.1	2.1
A2011Mar_08-09	14	28	22, 94	Trough	Inland	−76.8	−11.21	12.9	1.5
B2011Mar_08-09	25	46.6	22, 94	Trough	Inland	−84.9	−12.41	14.4	1.8
A2011Mar_20	10	20	22, 86	Trough	Inland	−86.8	−12.06	9.6	1.4
A2011Apr_09-10	6	11.8	15, 71	Cold front	Multiple directions	−12.6	−4.01	19.5	3.6
B2011May_10-12	12	22.6	14, 83	Cold front	SW	−6.5	−2.71	15.2	3.6
A2011Jul_04-06	15	28	11, 80	Cold front	WSW	−21.1	−5.18	20.3	2.4

[a]The ID is composed of sampling site (A for the Flinders campus, and B for Bridgewater), year, month, and day.
[b]The number of sampling vials. It only applies for the samples collected by the intraevent samplers. Most vials were prescribed to collect a maximum of 2 mm each, whereas a few were set to collect 1 mm each.
[c]Average air temperature and RH at Kent Town weather station during the rainfall period. For event samplers, a period of 24 h starting at 9 A.M. was used to calculate the average.
[d]Symbols used for oceanic air parcels: W for westerly, SW for southwesterly, and WSW in between.
[e]Standard deviation of intraevent deuterium excess.

between the two sites. For precipitation between April and October, the average *d*-excess was 17.9‰ at Bridgewater and 14.2‰ at the Flinders campus. Because the events sampled for the present study were mostly the result of large precipitation events, the difference in *d*-excess between Bridgewater and the Flinders campus site is small. For five events in which samples were collected from both sites, the average difference was only 1‰, which is in the range of analytical uncertainty for δ^2H (Table 1). Thus, the uncertainty in the data analysis resulting from the spatial variation between the two sites is considered very minor. Temperature and RH observed at Kent Town are also included in Table 1.

[24] In addition to stable isotope analyses, HYSPLIT backward trajectory analysis was performed for each of the 20 events to retrieve 48 h backward trajectories. The HYSPLIT modeling using two meteorological datasets (NCEP/NCAR and BOM) show similar results (with demonstration for one event included in Figure 7). Those resulting from NCEP/NCAR reanalysis data are reported because these data have a higher temporal resolution. For most events, the backward tracks were consistent among the six vertical levels. The results are summarized in Table 1.

[25] Eleven of the 20 events resulted from cold frontal systems. The surface RH was mostly approximately 70% to 80% during these frontal events. For such events, the moisture source for precipitation tends to be stable, generally westerly to southwesterly from the ocean. One selected event on 29 August 2009 is detailed in Figure 5. Between 9 A.M. of 29 August and 9 A.M. of 30 August, a total of 6.6 mm of rainfall was measured at Kent Town station. The collectors at sites A and B obtained 6.4 and 6.6 mm, respectively. Although the measured isotopic compositions (δ^2H and $\delta^{18}O$) of this event collected at the two sites are quite different, the deuterium excess is almost the same, and was as high as 22.5‰ (Table 1). The HYSPLIT modeling result indicates that the moisture source for this precipitation came from the west, primarily over the Great Australian Bight.

[26] Five of the 20 events resulted from synoptic low-pressure systems. For such events, backward air parcel trajectory analysis indicates that moisture sources were from inland or a mixture of inland and oceanic sources. One selected event on 3 and 4 September 2010 is detailed in Figure 6. Between 9 A.M. of 3 September and 9 A.M. of 5 September, a total of 38 mm of rainfall was measured at Kent Town station, whereas 36 mm of precipitation was collected at site A for this event. The measured deuterium excess of this event at site A was 10.4‰, with a large intraevent variability (coefficient of variation = 45%). The backward trajectory analysis results from HYSPLIT suggest that the moisture source of this event came from inland, spreading from northeasterly to northwesterly (Figure 6).

[27] The remaining four events resulted from large-scale trough systems. The moisture source of such an event tends to be from inland. During a trough or a convective event, RH in the subcloud layer is high, which is inferred from the

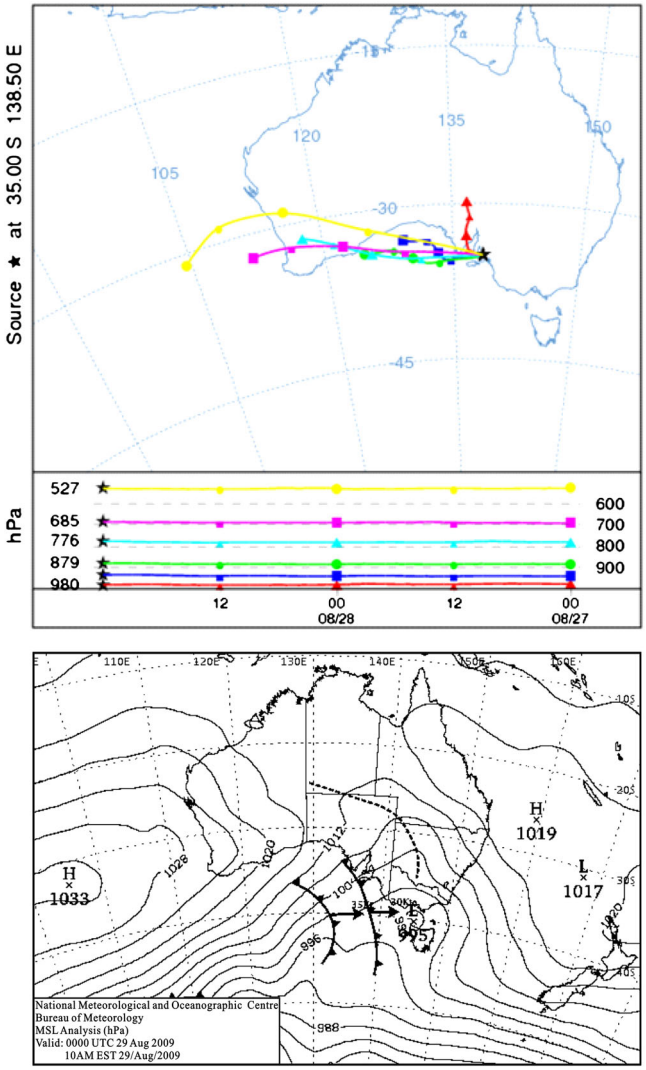

Figure 5. Example of a cold frontal system—synoptic weather chart at the mean sea level provided by BOM, and HYSPLIT-generated 48 h backward trajectories of air parcels at six vertical levels (100, 500, 1000, 2000, 3000, and 5000 m above ground level) for the 29 August 2009 event. Trajectories are based on NCEP/NCAR data.

near-surface observation during the event (Table 1). One selected event occurring on 8 March 2011 is detailed in Figure 7, with HYSPLIT results from both NCEP/NCAR and BOM meteorological data being shown together. The event was powered by a continental-scale trough system, connecting three low-pressure centers surrounding the Australian continent. For this event, from 9 A.M. of 8 March to 9 A.M. of 9 March, a total precipitation of 27.6 mm was measured at Kent Town. Rain samples of 28 and 46.6 mm were collected at sites A and B, respectively. The values of δ^2H and $\delta^{18}O$ were very low, with a deuterium excess of 13.8‰ (weighted average of the two sites). From the back-trajectory analysis, we infer that the moisture source for this event came northeasterly from inland (Figure 7).

[28] The deuterium excess of 10 frontal events with relatively stable oceanic moisture sources were plotted in Figure 8a. The *d*-excess standard deviation of intraevent samples ranges from 2.4‰ to 3.9‰ (Table 1). Generally, a westerly moisture source tends to be associated with a high deuterium excess in the resultant rainfall, with an average of 22.6‰ for the three events of such a moisture source direction. One event with a southwesterly moisture source had a low deuterium excess of approximately15.2‰. Events between westerly and southwesterly moisture sources consistently have a deuterium excess between approximately 15‰ and 20‰, with an average of 18.5‰.

[29] Deuterium excess of three large-scale trough events and three synoptic low-pressure systems with inland moisture sources in the lower troposphere are summarized in Figure 8b. Events of mixed moisture sources are not included to avoid moisture source effects in the variation of deuterium excess data. The three trough events have deuterium excesses of ≤15‰ (Figure 8b), with a *d*-excess standard deviation of intraevent samples ranging from

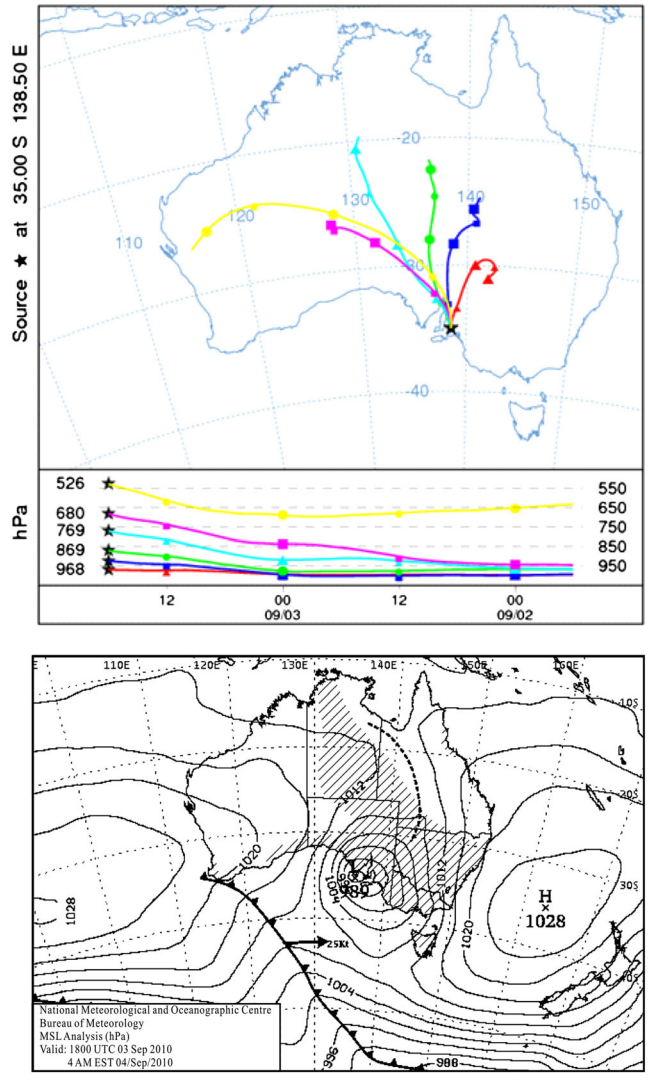

Figure 6. Example of a synoptic low-pressure system—synoptic weather chart at the mean sea level provided by BOM and HYSPLIT-generated 48 h backward trajectories of air parcels at six vertical levels (100, 500, 1000, 2000, 3000, and 5000 m above ground level) for the event occurring on 3 and 4 September 2010. Trajectories are based on NCEP/NCAR data.

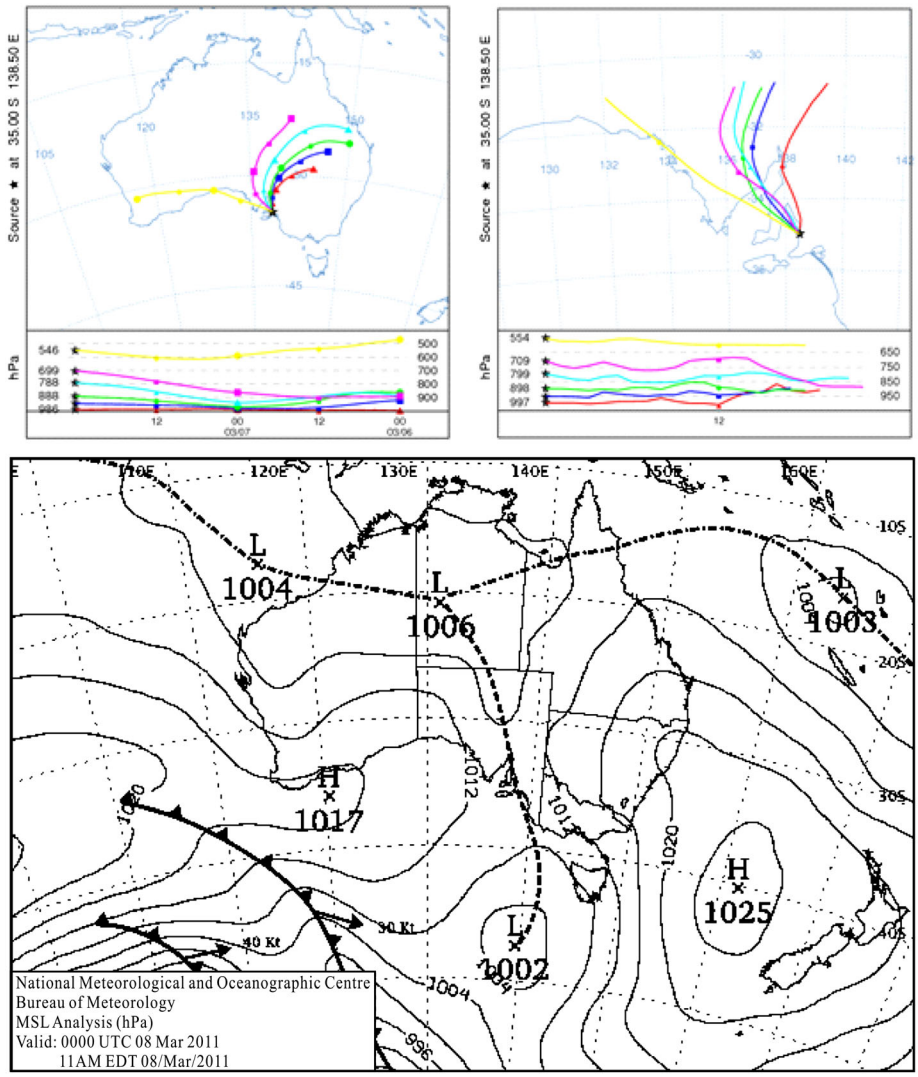

Figure 7. Example of a large-scale trough system—synoptic weather chart at the mean sea level provided by BOM and HYSPLIT-generated 48 h backward trajectories of air parcels at six vertical levels (100, 500, 1000, 2000, 3000, and 5000 m above ground level) for the 8 March 2011 event. Trajectories are based on NCEP/NCAR data (left) and BOM data (right).

1.4‰ to 5.6‰. The three convective events have a low deuterium excess, with a value of approximately 10‰, and a *d*-excess standard deviation of intraevent samples ranging from 2.5‰ to 13.4‰.

4. Discussion

4.1. Deuterium Excess and Synoptic Weather Patterns

[30] Deuterium excess of the precipitation resulting from low-pressure and trough systems are significantly lower than that resulting from cold frontal systems (Figure 8). This difference can occur in the same month (Figures 4a and 8), indicating that the difference between event types is not related to a seasonal change of temperature or a gradual shift of moisture sources, but rather is associated with different physical processes among the event types. Rainfall events resulting from synoptic scale low-pressure and trough systems have a deuterium excess of ≤15‰, and tend to have inland moisture sources (Table 1). Those due to low pressures often have a larger intraevent variability of deuterium excess. During a convective or trough system, vertical mixing of vapor and condensate tends to be stronger than during a frontal system. Several models and observations suggest that deuterium excess likely increases with elevation in the troposphere [*Bony et al*., 2008; *Masson-Delmotte et al*., 2008; *Sayres et al*., 2010]. If this is the case, vertical mixing importing moisture from higher altitudes would result in a higher deuterium excess in the precipitation. Thus, this mechanism does not explain the low *d*-excess in precipitation resulting from the convective and trough systems in this study.

[31] Thus, other mechanisms must have accounted for the low *d*-excess in precipitation resulting from the convective and trough systems. First, the inland moisture source may have a low deuterium excess. In tropical humid areas, inland moisture from surface water evaporation tends to increase deuterium excess of atmospheric moisture [*Gat and Matsui*, 1991]. However, in dry climate regions, evaporation rates quickly decrease right after rainfall events. In most instances, the local surface moisture contribution is mainly

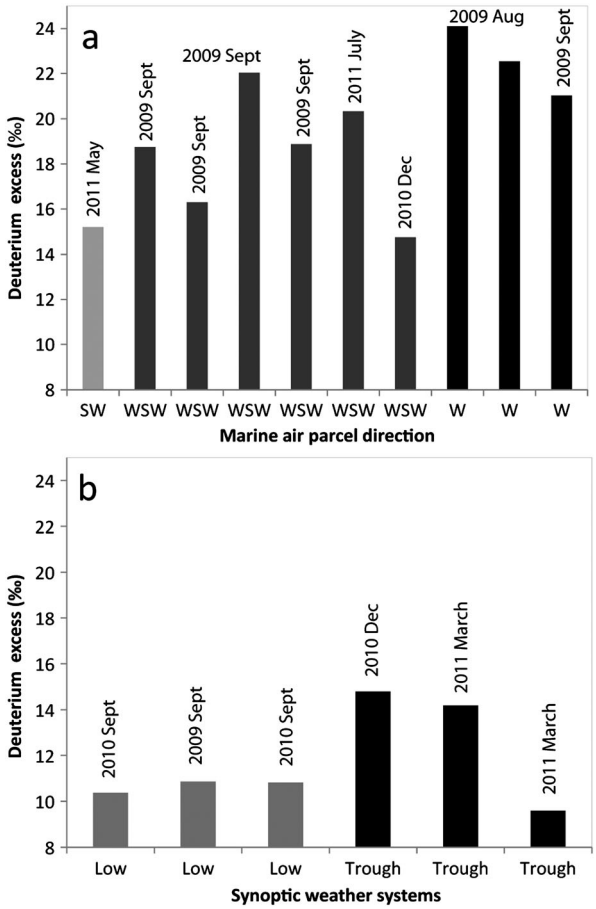

Figure 8. Deuterium excess of event rainwater for cold frontal systems (a) with different marine air parcel directions, and for events of inland-source air parcels (b) with different synoptic weather patterns (the values of some events are weighted averages of sites A and B, shown in Table 1). Events A2011Apr09-10, A2011Feb11, A2009Sep21, and B2011Jan13-14 are not included because multiple moisture source directions are indicated from the backward trajectory analysis for these events.

from plant transpiration of soil moisture, which tends to have a low deuterium excess [*Gat and Alrey*, 2006]. This mechanism was considered as a possible cause for the lower *d*-excess correlating with the higher convective activity in Niger [*Risi et al*., 2008b].

[32] Second, in a continental-scale low-pressure or trough system, precipitation water may result from a mixture of vapor over a much greater range than a cold frontal system. It is likely that the synoptic system integrates moisture sources from a wide latitudinal range. In the summer, the deuterium excess in the atmospheric moisture at high latitudes is near or below zero (Figure 9). This also occurs in the northern hemisphere, inferred from a rainfall isotope study in Canada [*Peng et al*., 2007]. This mechanism is supported by an event on 13 January 2011, in which a combination of inland and southerly moisture sources (from high latitudes) resulted in a *d*-excess of 0‰.

[33] Third, subcloud processes may contribute to low *d*-excess in the resultant precipitation as well. During a low-pressure or trough event, RH in the subcloud layer tends to be high. For nine low-pressure and trough events, the average RH at Kent Town was 87% (Table 1). The effective RH in the subcloud layer should be even higher [*Yoshimura et al*., 2010]. At such a high RH, the moisture exchange effect is more dominant than evaporation (Figure 1d). Thus, a low *d*-excess ambient vapor in the subcloud layer is needed to keep a low *d*-excess in precipitation.

[34] All three mechanisms are consistent with low *d*-excess moisture sources for a low-pressure or trough event in the study area. In addition to converging large-scale moisture sources, a low-pressure or trough system may recycle moisture during the event. In a convective system, modeling suggests that a large amount (~40%) of subcloud vapor originates from downdrafts that recycle the residual vapor at high altitude in the convective system and raindrop re-evaporation in the unsaturated downdraft column, and feed them back into the convective system [*Risi et al*., 2008a]. This downdraft recycling tends to cause a more depleted isotopic composition [*Risi et al*., 2008a], which is supported by the low $\delta^{18}O$ and $\delta^{2}H$ in quite a few such events (Table 1). Re-evaporation of raindrops in the unsaturated downdraft may also contribute to the low *d*-excess in the resulting precipitation.

[35] Without isotope-incorporated atmospheric modeling, it is difficult to evaluate the relative importance of these

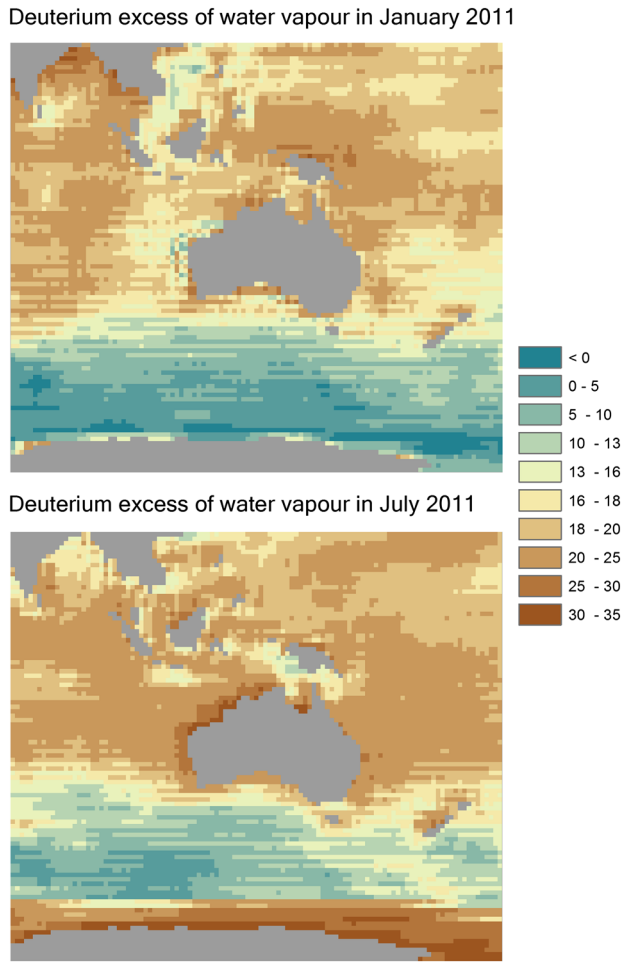

Figure 9. Deuterium excess of water vapor resulted from ocean evaporation, calculated based on equation (2), according to *Uemura et al*. [2008].

mechanisms in the resulting low precipitation deuterium excess [*Yoshimura et al*., 2010]. Measurements of vapor isotopic compositions are also helpful to investigate the effects of these mechanisms [*Tremoy et al*., 2012]. The recent development of measuring techniques, such as the wavelength-scanned cavity ring-down spectroscopy, provides a good opportunity to monitor moisture isotopes in the atmosphere [*Gupta et al*., 2009]. Although the exact mechanisms are not certain, in this study area, synoptic low-pressure and trough systems tend to result in a lower deuterium excess in rainfall compared with frontal systems. In contrast, precipitation resulting from a frontal system tends to have a larger *d*-excess, with a magnitude depending on oceanic moisture source directions (details to be given in the next section). This difference in precipitation *d*-excess between event types suggests that deuterium excess has the potential to retrieve (any records of) past occurrences of synoptic weather patterns. More discussion on this subject is included in section 4.5.

[36] The categorization of precipitation event types is useful to examine the synoptic weather system's effects on precipitation deuterium excess between an average frontal system and an average low-pressure or trough system. However, *d*-excess effects from the examined low-pressure and trough systems are not distinguishable from each other. This calls for a more appropriate categorization of synoptic weather systems for the study area. The organization degree of convective systems has been used in other areas to categorize both convective and low trough systems [*Risi et al*., 2008b; *Fudeyasu et al*., 2011], which may apply for the study area as well, and is worth further investigation. Moreover, it should be noted that the systemic difference in *d*-excess between frontal and low-pressure events observed in Adelaide in this study does not seem to agree with those observed in Melbourne [*Barras and Simmonds*, 2009]. However, *Barras and Simmonds* [2009] investigated only three events. More event-based measurements across a larger area in Australia will be helpful to resolve this apparent inconsistence.

4.2. Deuterium Excess and Oceanic Moisture Sources for Frontal Precipitation

[37] In the study area, rainfall events as a result of frontal systems tend to have a moisture source from the Indian Ocean to the south of Australia, with different path directions. Deuterium excess values in such events increase from southwesterly to westerly moisture sources (~15‰ to >20‰). This is consistent with the vapor deuterium excess in the source ocean surface, from below 16‰ to the southwest to above 20‰ to the west of the study area (Figure 9). In the Indian Ocean to the south of Australia, deuterium excess of water vapor decreases from low latitudes to high latitudes, and this trend is similar in summer and winter, as shown in two representative monthly maps of vapor deuterium excess (Figure 9). Overall, the deuterium excess in winter is slightly higher than that in summer over the majority of this part of the Indian Ocean, except for the Great Australian Bight. In the Great Australian Bight, to the west of Adelaide, deuterium excess is approximately 20‰ in winter, whereas the summer value is slightly higher (20‰–25‰). In the ocean to the southwest of Adelaide, deuterium excess ranges from more than 15‰ to less than 10‰, depending on the distance to Adelaide and the time of the year (Figure 9).

[38] In Adelaide, moisture source directions for mean monthly precipitation tend to be southwesterly in the summers to nearly westerly in the winters [*Guan et al*., 2009]. Such a seasonal shift in moisture source direction should at least partially cause the higher deuterium excess in winter rainfall than in the summer (Figure 9).

4.3. Deuterium Excess and Subcloud Processes

[39] Deuterium excess in raindrops can be altered by subcloud evaporation (i.e., evaporation of falling raindrops) and moisture exchange (Figure 1). Without measurements of the vapor isotopes' vertical profile, together with a humidity profile, it is difficult to distinguish the effects of evaporation and moisture isotope exchange in the subcloud layer. The following discussion will lump the two processes into one. The intraevent rain samples provide good information for examining the effect of subcloud processes on deuterium excess. Various plots of isotopic composition of intraevent samples for A2009Sep_25 (a frontal system), A2010Sep_03 (a low-pressure system), and A2011Mar_08 (a trough) are shown in Figure 10. The A2009Sep_25 event was driven by a cold frontal system, with a west-southwesterly oceanic moisture source. The first three samples were more enriched in heavy isotopes (less negative δ^2H and $\delta^{18}O$). Both weak rainout and strong subcloud evaporation could have accounted for this enriched isotopic composition in the early stage of the event. If we assume that the deuterium excess of source moisture was constant, the intraevent variability of deuterium excess was more likely due to the result of the subcloud processes, in particular, at the beginning of a rainfall event, given that the effect of condensation temperature variation is much smaller than that of subcloud processes (Figure 1). The first two vials collected precipitation at the beginning of the event, which often experiences subcloud evaporation, and had a low deuterium excess (Figure 10a). Similar phenomena are reported elsewhere [*Risi et al*., 2008a; *Barras and Simmonds*, 2009; *Yoshimura et al*., 2010; *Risi et al*., 2010b]. The rainwater in vials 4 and 5 were collected in the middle of the event. The rainfall intensity was high and therefore the subcloud evaporation was minimal; deuterium excess was thus least altered from the cloud. The sixth sample was collected over an approximately 3 h period in the afternoon, during which the subcloud evaporation was likely occurring, leading to a lower deuterium excess than vials 4 and 5. The last sample was collected within 1 h in the early evening. Significant subcloud evaporation was less likely. Thus, the deuterium excess returns to the level of the fourth and fifth samples. The reduced deuterium excess at the early stage of precipitation is also observed for most events sampled in this study, with two events of different synoptic types shown in Figures 10b and 10c. If the above interpretation is correct, and the vertical mixing of moisture can be neglected in the frontal event, deuterium excess of vials 4, 5, and 7, after the minor condensation temperature effect was corrected, should preserve the deuterium excess value of the moisture source. This discussion also suggests that the effect of subcloud evaporation is less important for a large event because the subcloud evaporation tends to be larger at the early stage of the rainfall, and is less important for a similar event of high rainfall intensity.

[40] The effect of subcloud evaporation is further evident in Figure 11, where the event deuterium excess values are

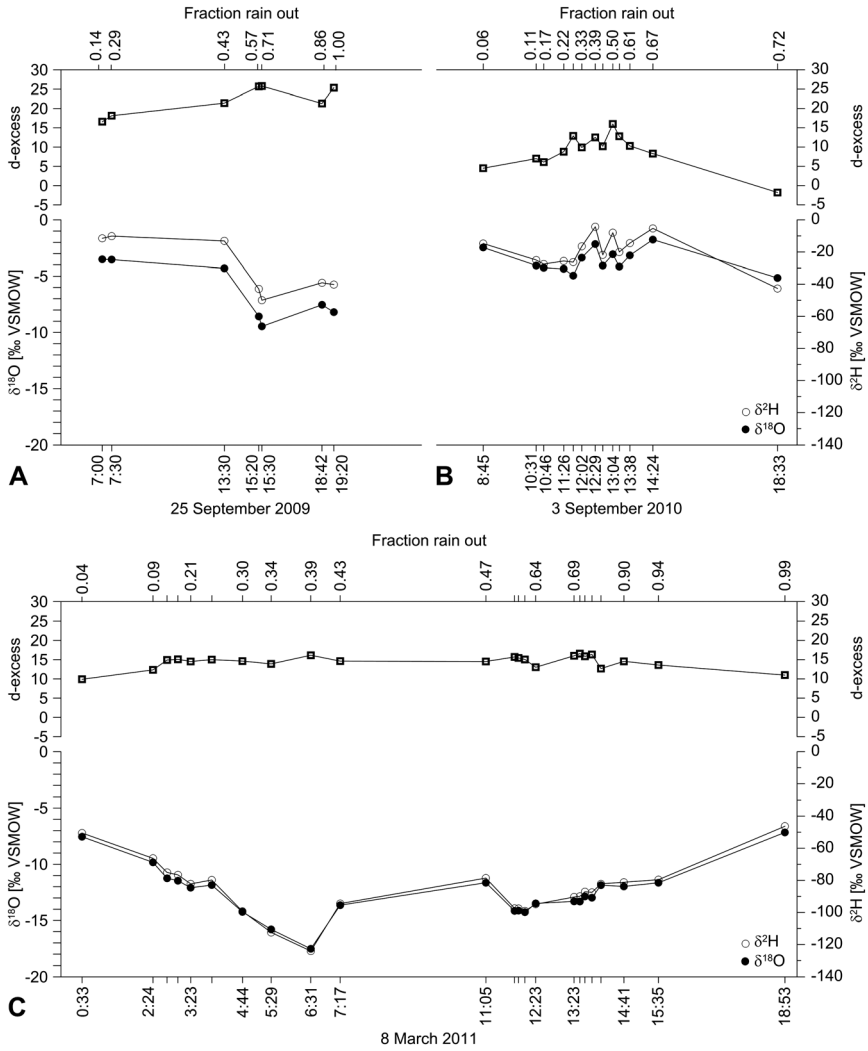

Figure 10. Intraevent variation of stable hydrogen and oxygen isotopic composition and deuterium excess as the precipitation progresses during three selected events: a frontal system (a), a low-pressure system (b), and a trough system (c) at the Flinders University campus site.

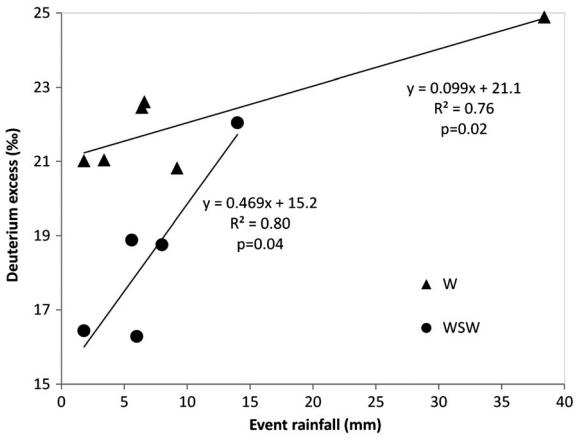

Figure 11. Deuterium excess versus event rainfall amount for the events of westerly moisture source (W, with the samples collected in late winter), and the events of the moisture source directions between westerly and southwesterly (WSW, with the samples collected in early spring).

plotted against the amount of rainfall for frontal events of similar oceanic moisture source area. A similar method has been used in *Peng et al*. [2007] to examine the subcloud evaporation effects, in which the isotopic composition of two groups of rainfall events of different amounts (smaller or larger than 4 mm) are compared. The events of the westerly moisture sources occurred in late August and early September (late winter). The events of the west-southwesterly moisture sources occurred in September (early spring; one event that occurred in December is not used in the plot to avoid the effects resulting from the different temperature and humidity conditions). For both groups of events, deuterium excess increases with rainfall amount, consistent with the hypothesis that the subcloud evaporation effects on the event-rainfall deuterium excess are smaller for a larger rainfall event. During more intense events, δ^2H and $\delta^{18}O$ decrease more strongly in the vapor phase due to raindrop re-evaporation or diffusive exchanges between raindrops and the ambient vapor [*Lawrence et al*., 2004; *Worden et al*., 2007; *Field et al*., 2010]. Because these two processes also act to increase *d*-excess in the vapor, we expect *d*-excess to increase

more strongly in the vapor phase during more intense events. Moisture exchange with such ambient vapor keeps the resultant precipitation *d*-excess close to the cloud-base precipitation (Figure 1d). Meanwhile, intense events may involve condensation at a lower temperature, and mix high *d*-excess moisture at higher elevations. Both tend to cause a higher *d*-excess in resultant precipitation.

[41] Within each group in Figure 11, because the source moisture came from a similar direction during a similar time of the year, it is reasonable to assume that they had similar deuterium excess in cloud water. The lower deuterium excess for a smaller rainfall was very likely owing to the relatively large subcloud evaporation. In comparison, a group of westerly moisture sources, occurring at the end of the winter season, is less sensitive to the amount of rainfall than the other groups occurring in spring. This is consistent with subcloud evaporation becoming more significant when the climate becomes drier and warmer as it progresses from winter to spring.

4.4. Subcloud Evaporation Inferred From GNIP Data

[42] The oxygen and hydrogen isotopic compositions are sensitive to both rainout fraction and subcloud evaporation. The deuterium excess in rainwater is sensitive to moisture sources, and decreases with subcloud evaporation, but it is less sensitive to rainout fraction (Figure 1a). Thus, the combination of either oxygen or hydrogen isotopic composition and deuterium excess is useful to examine subcloud evaporation (details explained in the methodology section). Based on this, subcloud evaporation is important in rainwater isotope compositions in the study area for October, November, December, February, and March (Figure 2b), when deuterium excess ($\delta^{18}O$) for weighted means is higher (lower) than that for arithmetic means. This effect could also be expected for January because January has similar temperature and humidity regime as December and February (Figure 4b). This is supported by the higher arithmetic mean $\delta^{18}O$ than the weighted mean observed for this month (Figure 2a). However, for deuterium excess, the arithmetic mean for this month is not smaller than the weighted mean as it is expected to be. An abrupt change in synoptic precipitation pattern, discussed in the next section, may resolve this inconsistency. Overall, deuterium excess and $\delta^{18}O$ of the multiple-year average monthly data confirm that the isotopic effects of subcloud processes is minor for May to September, and significant for October to April.

[43] However, it should be noted that in addition to a lower subcloud evaporation for large events, some other mechanisms, such as a stronger vertical moisture mixing in the cloud layer, or moisture recycling, may cause a higher *d*-excess in the resultant precipitation, which is difficult to discuss with monthly GNIP data, but covered in the previous three subsections on the event data.

4.5. Seasonal Variability of Deuterium Excess Inferred From Both GNIP and the Event Data

[44] In the study area, the deuterium excess is higher in wet winter months, and lower in dry summer months (Figure 2b). In winter, the frontal system is the dominant mechanism for rainfall in the area because the subtropical ridge moves northward inland. In summer, convective systems occur more frequently [*Ferguson and Wood*, 2011], leading to a significant amount of precipitation originating from the low-pressure and trough systems (Figure 12). This seasonal change in frequency of the frontal events and the low-pressure and trough events throughout the year contributes to the observed seasonal pattern of excess deuterium in the precipitation (Figure 2b).

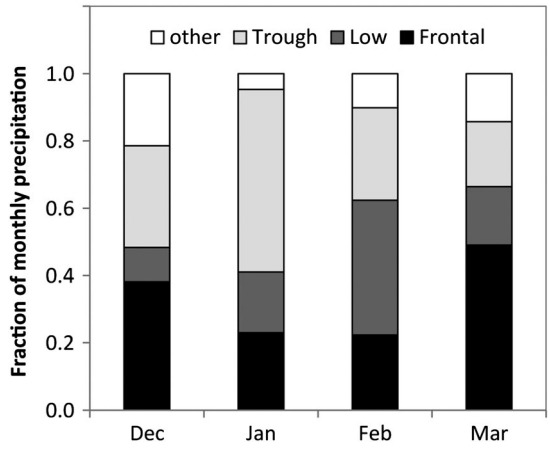

Figure 12. The fractions of monthly precipitation resulting from different synoptic weather systems for December, January, February, and March from the years 2000 to 2011, showing that low-pressure and trough systems result in 70% total precipitation in January and February, in comparison to a contribution of 40% in December and March.

[45] In addition, a gradual seasonal shift in oceanic moisture source direction for frontal events may also contribute to the seasonal deuterium excess pattern. From winter (June–August) to spring (September–November), moisture source directions gradually shift from westerly to southwesterly. This is inferred from a spatial analysis of long-term mean monthly precipitation [*Guan et al*., 2009], and is evident in this study (Table 1). The three events with a westerly moisture source all occurred in August and early September. Five of the six events with a west-southwesterly moisture source occurred in September and October (Table 1). The effect of this gradual shift in moisture source on frontal precipitation isotopic composition is clearly shown in Figure 13b. This decreasing trend in deuterium excess is strengthened by an increase in subcloud evaporation (Figure 11).

[46] As discussed in the Introduction, an abrupt change in the isotopic composition of precipitation occurs in January and February (Figure 2a). This phenomenon is also evident in Figure 13, in which the GNIP data points of these 2 months are located away from a cluster of all other months. Examination of the event isotopic composition indicates that a large-scale trough with inland moisture sources tends to have both a low deuterium excess (10‰–15‰) and low $\delta^{18}O$ (−12‰). Similarly, synoptic low-pressure systems tend to have a low deuterium excess, and some also have a low $\delta^{18}O$ (e.g., B2011Jan_13-14; Table 1). Similar isotopic patterns have been observed in other areas for organized connective events [*Risi et al*., 2008b] and typhoons [*Xie et al*., 2011]. The abrupt change in isotopic patterns in January and February (Figures 2 and 12), is likely due to an increasing frequency of such large-scale trough and low-pressure systems. This assumption is supported by the fact that approximately 70% of the precipitation in January and

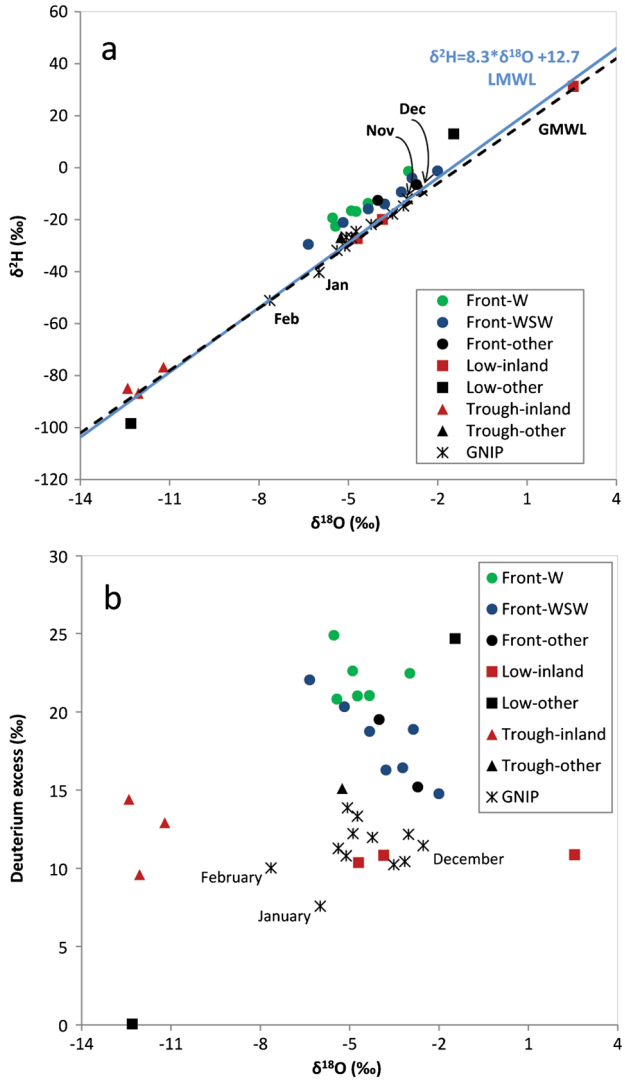

Figure 13. Plots of δ^2H versus $\delta^{18}O$ (a) and deuterium excess versus $\delta^{18}O$ (b) for events of three synoptic weather types: frontal (front), low-pressure (low), and trough (trough), with monthly mean data at GNIP Adelaide site for comparison. The moisture source direction is shown in the legend for the event data.

February between 2000 and 2011, measured at Kent Town, Adelaide (Figure 3) originated from such low-pressure and trough systems, in comparison to only 40% in December and March (Figure 12). An isotopic signature with low *d*-excess and $\delta^{18}O$ values was reported in groundwater samples resulting from historical recharge in the study area [*Guan et al.*, 2009], which was previously attributed to a colder paleoclimate. The results from this present study suggest an optional interpretation. Those groundwater samples could have been recharged from the summer storms driven by large-scale low-pressure and trough systems. A similar isotopic signature is missing from the modern groundwater, which indicates that these large-scale convective systems may have been more frequent in the past. More studies are needed to prove or disprove this implication.

[47] Interestingly, all six low-pressure and trough events, having inland moisture source directions, plot closely on the global and local meteoric water lines (Figure 13a), and have a deuterium excess closer to the global average (Figure 13b). In contrast, all frontal events plot above the global and local meteoric water lines and have a deuterium excess much larger than the global average (Figure 13). They also have a smaller interevent variability in isotopic composition compared with low-pressure and trough events (Table 1). These different isotopic patterns between the synoptic event types should be considered to examine the seasonal variability of isotopic composition in the study area.

5. Conclusions

[48] In the study area, both synoptic weather systems and associated atmospheric moisture sources are shown to influence deuterium excess values in precipitation. Rain events caused by frontal systems tend to have moisture sources from the Indian Ocean to the south of Australia. They usually have deuterium excesses of 15‰ to 25‰, depending on the moisture source direction. Rain events caused by synoptic low-pressure and trough systems tend to have inland moisture sources, and have a deuterium excess of 10‰ to 15‰. In addition to weather systems and associated moisture sources, subcloud evaporation and moisture exchange alters the deuterium excess in the resulting precipitation, which is more significant in summers when it is warm and dry, as seen in both GNIP and the event data.

[49] These factors together contribute to the seasonal variability of deuterium excess in the study area. Higher deuterium excess values in winter than in summer is mainly due to different dominant synoptic weather systems, i.e., dominant frontal systems in winter and dominant low-pressure and trough systems in summer. A gradual shift in moisture directions for the frontal systems from westerly in the winter, to west-southwesterly and southwesterly in the spring and summer also contribute to a decrease in precipitation deuterium excess from winter to summer. Subcloud evaporation and moisture exchange are stronger in summer than in winter, which further strengthens the difference in deuterium excess between them.

[50] Deuterium excess of winter frontal precipitation, resulting from minimum subcloud evaporation, is useful to infer the oceanic moisture source direction. In other seasons, deuterium excess of frontal precipitation is more likely to be altered by subcloud processes, and a correction needs to be done to retrieve source area deuterium excess information. Nevertheless, if intraevent samples are available, the source cloud deuterium excess of frontal precipitation can be estimated from samples in the middle of the event, which have experienced little subcloud processes. The results from the analysis of GNIP data in Adelaide suggest that an abrupt change in dominant precipitation weather patterns in South Australia occurs in January and February, characterized by a sudden decrease in $\delta^{18}O$ and deuterium excess. This is likely caused by an increasing occurrence of large-scale trough and low-pressure systems in these 2 months.

[51] **Acknowledgment.** Peter Selva Raj, Lucas Wood, Chuanyu Zhu, Leighton Randell, and Yunhui Guo from Flinders University, and Yimin Huang and Huawu Wu from Hunan Normal University assisted in sample collection and some data preparation for this study. Constructive comments and suggestions from three anonymous reviewers significantly improved the manuscript. H. Guan is supported by the National Centre for Groundwater Research and Training funded by Australian Research Council and Water

Commission, and is supported by the Hunan Bairen Program, X. Zhang is supported by the Construct Program of the Key Discipline in Hunan Province of China, and G. Skrzypek is supported by Future Fellowship from Australian Research Council.

References

Allison, G. B., and C. J. Barnes (1983), Estimation of evaporation from non-vegetated surfaces using natural deuterium, *Nature*, *301*, 143–145.

Barras, V., and I. Simmonds (2009), Observation and modeling of stable water isotopes as diagnostics of rainfall dynamics over southeastern Australia, *J. Geophys. Res.*, *114*, D23308, doi: 10.1029/2009JD012132.

Blasch, K. W., and J. R. Bryson (2007), Distinguishing sources of ground water recharge by using delta H-2 and delta O-18, *Ground Water*, *45* (3), 294–308, doi: 10.1111/j.1745-6584.2006.00289.x.

Blisniuk, P. M., and L. A. Stern (2005), Stable isotope paleoaltimetry: A critical review, *Am. J. Sci.*, *305*(10), 1033–1074, doi: 10.2475/ajs.305.10.1033.

Bony, S., C. Risi, and F. Vimeux (2008), Influence of convective processes on the isotopic composition (delta O-18 and delta D) of precipitation and water vapor in the tropics: 1. Radiative-convective equilibrium and Tropical Ocean-Global Atmosphere-Coupled Ocean-Atmosphere Response Experiment (TOGA-COARE) simulations, *J. Geophys. Res*, *113*, D19305, doi: 10.1029/2008JD009942.

Bowen, G. J., and B. Wilkinson (2002), Spatial distribution of delta O-18 in meteoric precipitation, *Geology*, *30*(4), 315–318, doi: 10.1130/0091-7613.

Bowen, G. J., and J. Revenaugh (2003), Interpolating the isotopic composition of modern meteoric precipitation, *Water Resour. Res.*, *39*(10), 13, doi: 10.1029/2003wr002086.

Cappa, C. D., M. B. Hendricks, D. J. DePaolo, and R. C. Cohen (2003), Isotopic fractionation of water during evaporation, *J. Geophys. Res.*, *108*(D16), 4525, doi: 10.1029/2003JD003597.

Celle-Jeanton, H., R. Gonfiantini, Y. Travi, and B. Sol (2004), Oxygen-18 variations of rainwater during precipitation: application of the Rayleigh model to selected rainfalls in Southern France, *J. Hydrol.*, *289*(1–4), 165–177, doi: 10.1016/j.jhydrol.2003.11.017.

Craig, H. (1961), Isotopic variation in meteoric waters, *Science*, *133*, 1702–1703.

Dangela, D., and A. Longinelli (1990), Oxygen isotopes in living mammals bone phosphate—further results, *Chem. Geol.*, *86*(1), 75–82.

Dansgaard, W. (1964), Stable isotopes in precipitation, *Tellus*, *16*, 436–468.

Draxler, R., B. Stunder, G. Rolph, A. Stein, and A. Taylor (2009), HYSPLIT 4 User's Guide, NOAA, USA.

Ersek, V., A. C. Mix, and P. U. Clark (2010), Variations of delta O-18 in rainwater from southwestern Oregon, *J. Geophys. Res.*, *115*, D09109, doi: 10.1029/2009JD013345.

Ferguson, C. R., and E. F. Wood (2011), Observed Land-Atmosphere Coupling from Satellite Remote Sensing and Reanalysis, *J. Hydrometeorol.*, *12*(6), 1221–1254, doi: 10.1175/2011jhm1380.1.

Field, R. D. (2010), Observed and modeled controls on precipitation delta O-18 over Europe: From local temperature to the Northern Annular Mode, *J. Geophys. Res.*, *115*, doi: 10.1029/2009JD013370.

Field, R. D., D. B. A. Jones, and D. P. Brown (2010), Effects of postcondensation exchange on the isotopic composition of water in the atmosphere, *J. Geophys. Res.*, *115*, D24305, doi: 10.1029/2010JD014334.

Frankenberg, C., et al. (2009), Dynamic Processes Governing Lower-Tropospheric HDO/H2O Ratios as Observed from Space and Ground, *Science*, *325*(5946), 1374–1377, doi: 10.1126/science.1173791.

Friedman, I., G. I. Smith, J. D. Gleason, A. Warden, and J. M. Harris (1992), Stable isotope composition of waters in southeastern California. 1. Modern precipitation, *J. Geophys. Res.*, *97*(D5), 5795–5812.

Frot, E., B. van Wesemael, G. Vandenschrick, R. Souchez, and A. S. Benet (2007), Origin and type of rainfall for recharge of a karstic aquifer in the western Mediterranean: a case study from the Sierra de Gador-Campo de Dalias (southeast Spain), *Hydrol. Process.*, *21*(3), 359–368, doi: 10.1002/hyp.6238.

Fudeyasu, H., K. Ichiyanagi, K. Yoshimura, S. Mori, J. I. Hamada, N. Sakurai, M. D. Yamanaka, J. Matsumoto, and F. Syamsudin (2011), Effects of Large-scale Moisture Transport and Mesoscale Processes on Precipitation Isotope Ratios Observed at Sumatera, Indonesia, *J. Meteorol. Soc. Jpn.*, *89A*, 49–59, doi: 10.2151/jmsj.2011-A03.

Gat, J. R. (1996), Oxygen and hydrogen isotopes in the hydrologic cycle, *Annu. Rev. Earth Planet. Sci.*, *24*, 225–262.

Gat, J. R., and E. Matsui (1991), Atmospheric water-balance in the Amazon Basin—an isotopic evapotranspiration model, *J. Geophys. Res.*, *96*(D7), 13179–13188.

Gat, J. R., and P. L. Alrey (2006), Stable water isotopes in the atmosphere/biosphere/lithosphere interface: Scaling-up from the local to continental scale, under humid and dry conditions, *Glob. Planet. Change*, *51*(1–2), 25–33, doi: doi:10.1016/j.gloplacha.2005.12.004.

Guan, H., C. T. Simmons, and A. J. Love (2009), Orographic controls on rain water isotope distribution in the Mount Lofty Ranges of South Australia, *J. Hydrol.*, *374*(3–4), 255–264, doi: 10.1016/j.jhydrol.2009.06.018.

Guan, H., X. Zhang, O. Makhnin, and Z. Sun (2012), Mapping mean monthly temperatures over a coastal hilly area incorporating terrain aspect effects, *J. Hydrometeorol.*, doi: 10.1175/JHM-D-12-014.1.

Gupta, P., D. Noone, J. Galewsky, C. Sweeney, and B. H. Vaughn (2009), Demonstration of high-precision continuous measurements of water vapor isotopologues in laboratory and remote field deployments using wavelength-scanned cavity ring-down spectroscopy (WS-CRDS) technology, *Rapid Commun. Mass Spectrom.*, *23*(16), 2534–2542, doi: 10.1002/Rcm.4100.

Hoffmann, G., M. Werner, and M. Heimann (1998), Water isotope module of the ECHAM atmospheric general circulation model: A study on timescales from days to several years, *J. Geophys. Res.*, *103*(D14), 16871–16896.

Jones, P. D., et al. (2009), High-resolution palaeoclimatology of the last millennium: a review of current status and future prospects, *Holocene*, *19*(1), 3–49, doi: 10.1177/0959683608098952.

Joussaume, S., R. Sadourny, and J. Jouzel (1984), A general circulation model of water isotope cycles in the atmosphere, *Nature*, *311*(5981), 24–29.

Jouzel, J. (2003), Water stable isotopes: atmospheric composition and applications in polar ice core studies, *Treatise on Geochemistry*, *4*, 213–243, doi: 10.1016/B0-08-043751-6/04040-8.

Jouzel, J., K. Froehlich, and U. Schotterer (1997), Deuterium and oxygen-18 in present-day precipitation: data and modelling, *Hydrol. Sci. J.-J. Sci. Hydrol.*, *42*(5), 747–763.

Kalnay, E., et al. (1996), The NCEP/NCAR 40-year reanalysis project, *Bull. Amer. Meteorol. Soc.*, *77*(3), 437–471.

Kohn, M. J., and J. M. Welker (2005), On the temperature correlation of delta O-18 in modem precipitation, *Earth Planet. Sci. Lett.*, *231*(1–2), 87–96, doi: 10.1016/j.epsl.2004.12.004.

Krinner, G., C. Genthon, and J. Jouzel (1997), GCM analysis of local influences on ice core delta signals, *Geophys. Res. Lett.*, *24*(22), 2825–2828.

Lai, C. T., and J. Ehleringer (2011), Deuterium excess reveals diurnal sources of water vapor in forest air, *Oecologia*, *165*(1), 213–223, doi: 10.1007/s00442-010-1721-2.

Lawrence, J. R., S. D. Gedzelman, D. Dexheimer, H. K. Cho, G. D. Carrie, R. Gasparini, C. R. Anderson, K. P. Bowman, and M. I. Biggerstaff (2004), Stable isotopic composition of water vapor in the tropics, *J. Geophys. Res.*, *109*(D6), doi: 10.1029/2003jd004046.

Lee, J. E., I. Fung, D. J. DePaolo, and C. C. Henning (2007), Analysis of the global distribution of water isotopes using the NCAR atmospheric general circulation model, *J. Geophys. Res.*, *112*(D16), doi: 10.1029/2006jd007657.

Liebminger, A., G. Haberhauer, W. Papesch, and G. Heiss (2006), Correlation of the isotopic composition in precipitation with local conditions in alpine regions, *J. Geophys. Res.*, *111*(D5), doi:10.1029/2005jd006258.

Liotta, M., R. Favara, and M. Valenza (2006), Isotopic composition of the precipitations in the central Mediterranean: Origin marks and orographic precipitation effects, *J. Geophys. Res.*, *111*(D19), doi:10.1029/2005jd006818.

Liu, J. R., G. B. Fu, X. F. Song, S. P. Charles, Y. H. Zhang, D. M. Han, and S. Q. Wang (2010), Stable isotopic compositions in Australian precipitation, *J. Geophys. Res.*, *115*, D23307, doi: 10.1029/2010JD014403.

Masson-Delmotte, V., J. Jouzel, A. Landais, M. Stievenard, S. J. Johnsen, J. W. C. White, M. Werner, A. Sveinbjornsdottir, and K. Fuhrer (2005), GRIP deuterium excess reveals rapid and orbital-scale changes in Greenland moisture origin, *Science*, *309*(5731), 118–121, doi: 10.1126/science.1108575.

Masson-Delmotte, V., et al. (2011), Sensitivity of interglacial Greenland temperature and delta O-18: ice core data, orbital and increased CO2 climate simulations, *Clim. Past.*, *7*(3), 1041–1059, doi: 10.5194/cp-7-1041-2011.

Masson-Delmotte, V., et al. (2008), A review of Antarctic surface snow isotopic composition: Observations, atmospheric circulation, and isotopic modeling, *J. Clim.*, *21*(13), 3359–3387, doi: 10.1175/2007jcli2139.1.

Mathieu, R., D. Pollard, J. E. Cole, J. W. C. White, R. S. Webb, and S. L. Thompson (2002), Simulation of stable water isotope variations by the GENESIS GCM for modern conditions, *J. Geophys. Res.*, *107*(D4), 4037, doi: 10.1029/2001JD900255.

McCarroll, D., and N. J. Loader (2004), Stable isotopes in tree rings, *Quat. Sci. Rev.*, *23*(7–8), 771–801, doi: 10.1016/j.quascirev.2003.06.017.

McDermott, F. (2004), Palaeo-climate reconstruction from stable isotope variations in speleothems: a review, *Quat. Sci. Rev.*, *23*(7–8), 901–918, doi: 10.1016/j.quascirev.2003.06.021.

Merlivat, L., and J. Jouzel (1979), Global climatic interpretation of the deuterium-oxygen 18 relationship for precipitation, *J. Geophys. Res. 84* (C8), 5029–5033.

Moreira, M. Z., L. D. L. Sternberg, L. A. Martinelli, R. L. Victoria, E. M. Barbosa, L. C. M. Bonates, and D. C. Nepstad (1997), Contribution of transpiration to forest ambient vapour based on isotopic measurements, *Glob. Chang. Biol.*, *3*(5), 439–450.

Noone, D., and I. Simmonds (2002), Associations between delta O-18 of water and climate parameters in a simulation of atmospheric circulation for 1979-95, *J. Clim.*, *15*(22), 3150–3169, doi: 10.1175/1520-0442.

Pang, H. X., Y. Q. He, Z. L. Zhang, A. G. Lu, J. Gu, and J. D. Zhao (2005), Origin of summer monsoon rainfall identified by delta O-18 in precipitation, *Chin. Sci. Bull.*, *50*(23), 2761–2764, doi: 10.1360/982004-363.

Peng, H., B. Mayer, S. Harris, and H. R. Krouse (2007), The influence of below-cloud secondary effects on the stable isotope composition of hydrogen and oxygen in precipitation at Calgary, Alberta, Canada, *Tellus B Chem. Phys. Meteorol.*, *59*(4), 698–704, doi: 10.1111/j.1600-0889.2007.00291.x.

Pfahl, S., and H. Wernli (2008), Air parcel trajectory analysis of stable isotopes in water vapor in the eastern Mediterranean, *J. Geophys. Res.*, *113*, D20104, doi: 10.1029/2008JD009839.

Reynolds, R. W., N. A. Rayner, T. M. Smith, D. C. Stokes, and W. Q. Wang (2002), An improved in situ and satellite SST analysis for climate, *J. Clim.*, *15*(13), 1609–1625, doi: 10.1175/1520-0442.

Risi, C., S. Bony, and F. Vimeux (2008a), Influence of convective processes on the isotopic composition (delta(18)O and delta D) of precipitation and water vapor in the tropics: 2. Physical interpretation of the amount effect, *J. Geophys. Res.*, *113*, D19306, doi: 10.1029/2008JD009943.

Risi, C., S. Bony, F. Vimeux, and J. Jouzel (2010a), Water-stable isotopes in the LMDZ4 general circulation model: Model evaluation for present-day and past climates and applications to climatic interpretations of tropical isotopic records, *J. Geophys. Res.*, *115*, D12118, doi: 10.1029/2009JD013255.

Risi, C., S. Bony, F. Vimeux, M. Chong, and L. Descroix (2010b), Evolution of the stable water isotopic composition of the rain sampled along Sahelian squall lines, *Q. J. R. Meteorol. Soc.*, *136*, 227–242, doi: 10.1002/Qj.485.

Risi, C., S. Bony, F. Vimeux, C. Frankenberg, D. Noone, and J. Worden (2010c), Understanding the Sahelian water budget through the isotopic composition of water vapor and precipitation, *J. Geophys. Res.*, *115*, D24110, doi: 10.1029/2010JD014690.

Risi, C., S. Bony, F. Vimeux, L. Descroix, B. Ibrahim, E. Lebreton, I. Mamadou, and B. Sultan (2008b), What controls the isotopic composition of the African monsoon precipitation? Insights from event-based precipitation collected during the 2006 AMMA field campaign, *Geophys. Res. Lett.*, *35*, L24808, doi: 10.1029/2008GL035920.

Rozanski, K., L. Araguasaraguas, and R. Gonfiantini (1992), Relation between long-term trends of Oxygen-18 isotope composition of precipitation and climate, *Science*, *258*(5084), 981–985.

Rozanski, K., S. J. Johnsen, U. Schotterer, and L. G. Thompson (1997), Reconstruction of past climates from stable isotope records of palaeo-precipitation preserved in continental archives, *Hydrol. Sci. J.-J. Sci. Hydrol.*, *42*(5), 725–745.

Salati, E., A. Dallolio, E. Matsui, and J. R. Gat (1979), Recycling of water in the amazon basin—isotopic study, *Water Resour. Res.*, *15*(5), 1250–1258.

Sayres, D. S., L. Pfister, T. F. Hanisco, E. J. Moyer, J. B. Smith, J. M. St Clair, A. S. O'Brien, M. F. Witinski, M. Legg, and J. G. Anderson (2010), Influence of convection on the water isotopic composition of the tropical tropopause layer and tropical stratosphere, *J. Geophys. Res.*, *115*, doi: 10.1029/2009jd013100.

Sime, L. C., E. W. Wolff, K. I. C. Oliver, and J. C. Tindall (2009), Evidence for warmer interglacials in East Antarctic ice cores, *Nature*, *462*(7271), 342–U105, doi: 10.1038/08564.

Skrzypek, G., A. Wisniewski, and P. F. Grierson (2011), How cold was it for Neanderthals moving to Central Europe during warm phases of the last glaciation?, *Quat. Sci. Rev.*, *30*(5-6), 481–487, doi: 10.1016/j.quascirev.2010.12.018.

Stewart, M. K. (1975), Stabel isotope fractionation due to evaporation and isotope exchange of falling water drops: Application to atmospheric processes and evaporation of lakes, *J. Geophys. Res.*, *80*, 1133–1146.

Thompson, L. G., E. Mosley-Thompson, and K. A. Henderson (2000), Ice-core palaeoclimate records in tropical South America since the Last Glacial Maximum, *J. Quat. Sci.*, *15*(4), 377–394.

Tremoy, G., F. Vimeux, S. Mayaki, I. Souley, O. Cattani, C. Risi, G. Favreau, and M. Oi (2012), A 1-year long delta O-18 record of water vapor in Niamey (Niger) reveals insightful atmospheric processes at different timescales, *Geophys. Res. Lett.*, *39*, L08805, doi: 10.1029/2012GL051298.

Uemura, R., Y. Matsui, K. Yoshimura, H. Motoyama, and N. Yoshida (2008), Evidence of deuterium excess in water vapor as an indicator of ocean surface conditions, *J. Geophys. Res.*, *113*, D19114, doi: 10.1029/2008JD010209.

Vachon, R. W., J. M. Welker, J. W. C. White, and B. H. Vaughn (2010), Moisture source temperatures and precipitation delta(18)O-temperature relationships across the United States, *Water Resour. Res.*, *46*, W07523, doi: 10.1029/2009WR008558.

Vodila, G., L. Palcsu, I. Futo, and Z. Szanto (2011), A 9-year record of stable isotope ratios of precipitation in Eastern Hungary: Implications on isotope hydrology and regional palaeoclimatology, *J. Hydrol.*, *400* (1–2), 144–153, doi: 10.1016/j.jhydrol.2011.01.030.

Wang, L. X., K. K. Caylor, J. C. Villegas, G. A. Barron-Gafford, D. D. Breshears, and T. E. Huxman (2010), Partitioning evapotranspiration across gradients of woody plant cover: Assessment of a stable isotope technique, *Geophys. Res. Lett.*, *37*, L09401, doi: 10.1029/2010GL043228.

Wang, X. F., A. S. Auler, R. L. Edwards, H. Cheng, E. Ito, and M. Solheid (2006), Interhemispheric anti-phasing of rainfall during the last glacial period, *Quat. Sci. Rev.*, *25*(23–24), 3391–3403, doi: 10.1016/j.quascirev.2006.02.009.

Werner, M., M. Heimann, and G. Hoffmann (2001), Isotopic composition and origin of polar precipitation in present and glacial climate simulations, *Tellus B Chem. Phys. Meteorol.*, *53*(1), 53–71.

Williams, D. G., et al. (2004), Evapotranspiration components determined by stable isotope, sap flow and eddy covariance techniques, *Agric. For. Meteorol.*, *125*(3–4), 241–258, doi: 10.1016/j.agrformet.2004.04.008.

Worden, J., D. Noone, K. Bowman, and S. Tropospheric Emission (2007), Importance of rain evaporation and continental convection in the tropical water cycle, *Nature*, *445*(7127), 528–532, doi: 10.1038/nature05508.

Xie, L. H., G. J. Wei, W. F. Deng, and X. L. Zhao (2011), Daily delta O-18 and delta D of precipitations from 2007 to 2009 in Guangzhou, South China: Implications for changes of moisture sources, *J. Hydrol.*, *400*(3–4), 477–489, doi: 10.1016/j.jhydrol.2011.02.002.

Yakir, D., and L. D. L. Sternberg (2000), The use of stable isotopes to study ecosystem gas exchange, *Oecologia*, *123*(3), 297–311.

Yamanaka, T., J. Shimada, and K. Miyaoka (2002), Footprint analysis using event-based isotope data for identifying source area of precipitated water, *J. Geophys. Res.*, *107*(D22), 4624, doi: 10.1029/2001JD001187, 2002.

Yepez, E. A., D. G. Williams, R. L. Scott, and G. Lin (2003), Partitioning overstory and understory evapotranspiration in a semiarid savanna woodland from the isotopic composition of water vapor, *Agric. For. Meteorol.*, *119*(1–2), 53–68, doi: 10.1016/S0168-1923(03)00116-3.

Yoshimura, K., M. Kanamitsu, and M. Dettinger (2010), Regional downscaling for stable water isotopes: A case study of an atmospheric river event, *J. Geophys. Res.*, *115*, doi: 10.1029/2010jd014032.

Yoshimura, K., T. Oki, N. Ohte, and S. Kanae (2004), Colored moisture analysis estimates of variations in 1998 Asian monsoon water sources, *J. Meteorol. Soc. Jpn.*, *82*(5), 1315–1329, doi: 10.2151/jmsj.2004.1315.

Zhang, X. P., J. M. Liu, X. Y. Wang, M. Nakawo, Z. C. Xie, J. M. Zhang, and X. Z. Zhang (2010), Climatological significance of stable isotopes in precipitation over south-west China, *Int. J. Climatol.*, *30*(14), 2229–2239, doi: 10.1002/Joc.2037.